

Towards Numerical Simulations of Atherosclerosis: Modelling of Low-Density-Lipoprotein (LDL) Transport through Multi-Layered Arterial Wall

A. de Loor¹ and S. Kenjereš¹

¹ Faculty of Applied Sciences, Delft University of Technology, Delft, The Netherlands

Abstract— The high concentration of the low-density-lipoprotein (LDL) is recognised as one of the principal risk factors for development of the atherosclerosis. The paper reports on modelling and simulations of the LDL transport through the multi-layered patient-specific arterial wall. The mathematical model includes conservative equations of mass, momentum and concentration that are specifically re-derived to include a porous layer structure, effects of the biological membranes and reactive source/sink terms in different layers of the arterial wall. Then, a four-layer wall model is introduced and firstly tested on a simple cylinder geometry where realistic layer properties are specified. Comparative assessment with results presented in Yang and Vafai [4] proved proper implementation of the mathematical model. Excellent agreement for the velocity and LDL concentration distributions in the artery lumen and in the artery wall are obtained. Then, a patient-specific carotid artery bifurcation is studied. We found a strong dependency between underlying blood flow pattern (and consequently the wall-shear-stress (WSS) distributions) and the uptake of the LDL concentration in the artery wall. The radial dependency of interactions between the diffusion, convection and chemical reaction within the multi-layered artery wall is crucial for accurate predictions of the LDL in the media. It is demonstrated that a four-layer wall model represents a good platform for the future numerical investigations of atherosclerosis for the patient-specific geometries.

Keywords— atherosclerosis, LDL transport, multi-layered artery wall

I. INTRODUCTION

The process of forming atheromous plaques in the inner lining of arteries (atherosclerosis) is complex process, but one of the principal risk factors is high concentration of cholesterol in the blood plasma, especially low-density-lipoprotein (LDL) cholesterol. Atherosclerosis primarily occurs in large- and medium-sized arteries, like the coronary and carotid arteries, especially at bifurcations and curvatures, [1], [2]. Although a series of cellular and molecular responses is involved in the process, the uptake of the LDL in the artery

wall plays a key role, [2]. The uptake of LDL in the artery wall will enhance the inflammatory response. Although the entire process behind this disease is not yet completely understood, several models have been developed to calculate the mass transport to the artery wall, [3]. Three categories of models can be identified: wall-free, lumen-wall and multi-layer models. In the first, the artery wall is modelled as a boundary layer, in the second the artery wall is one homogeneous layer and in the latter the arterial wall is divided into multiple layers. The latter type of models is the most realistic as it takes into account the non-homogenous structure of the artery wall. However, it also needs the largest number of transport parameters and requires quite challenging numerical mesh generation. In this study, we focus on this third class of the wall-model proposed by [4]. The goal of our study is to simulate the transport of the LDL into the artery wall of a patient-specific carotid bifurcation in order to be able to locate those areas that are at high risk of developing atherosclerosis.

II. MATHEMATICAL MODEL

In addition to the conservation equations of mass and momentum of blood flow in the lumen, additional equations for transport of the blood plasma and of the LDL concentration through a multi-layer artery wall are introduced. They are based on a combination of a porous layer and a biological membrane equations with a chemical reaction source/sink term, [4]. The volume-averaged momentum equation can be written as

$$\frac{\rho}{\varepsilon} \frac{\partial \langle \vec{v} \rangle}{\partial t} + \frac{\rho}{\varepsilon} \langle (\vec{v} \cdot \nabla) \vec{v} \rangle = -\frac{\nabla \langle p \rangle}{\varepsilon} + \nabla \cdot \frac{\mu}{\varepsilon} \nabla \langle \vec{v} \rangle - \frac{\mu}{K} \langle \vec{v} \rangle + \sigma RT \nabla \langle c \rangle \quad (1)$$

where ρ is the density, μ the dynamical viscosity, ε is the porosity, K the permeability, σ is the reflection coefficient, T is temperature and R the universal gas constant. The third term on the right-hand side is the flow resistance by the solid matrix of a porous medium given by Darcy's law and the fourth term is the osmotic pressure term. Similarly, the

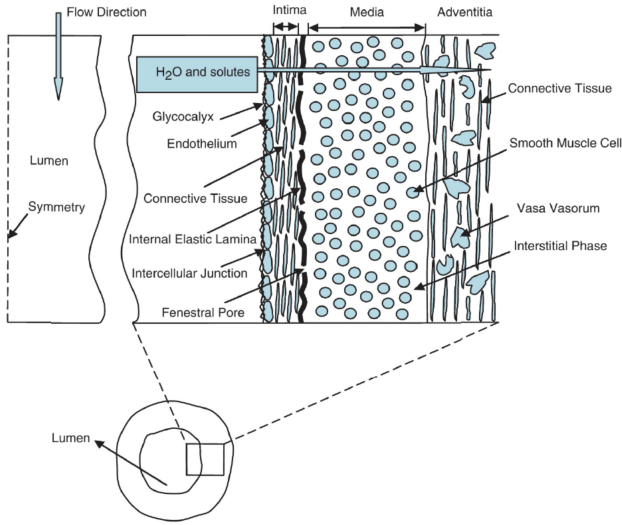


Fig. 1: Schematic representation of the multi-layered structure of an artery wall, [4].

Table 1: Characteristic thickness of the artery wall layers.

Wall layer	Thickness (μm)
Endothelium	2.0
Intima	10.0
Internal Elastic Layer (IEL)	2.0
Media	200.0

volume-averaged convective-diffusive-reactive mass transport equation can be written as

$$\frac{\partial \langle c \rangle}{\partial t} + (1 - \sigma) \langle \vec{v} \rangle \cdot \nabla \langle c \rangle = \mathcal{D}_e \nabla^2 \langle c \rangle + k_{react} \langle c \rangle \quad (2)$$

where k_{react} is the effective volumetric reaction rate coefficient. A schematic representation of here adopted four-layer wall model is shown in Fig. 1. An overview of the characteristic thickness of the artery wall-layers is shown in Tab. 1.

III. RESULTS AND DISCUSSION

Before the carotid artery bifurcation simulations, numerical implementation of the mathematical model given by Eqs.(1) and (2) is validated against simplified two-dimensional (polar-cylindrical) and three-dimensional (full cylinder) geometries and an excellent agreement with results presented in [4] are obtained, Fig. 2. These results are obtained by using a numerical mesh with 800 control volumes in the radial direction. The results for the velocity magni-

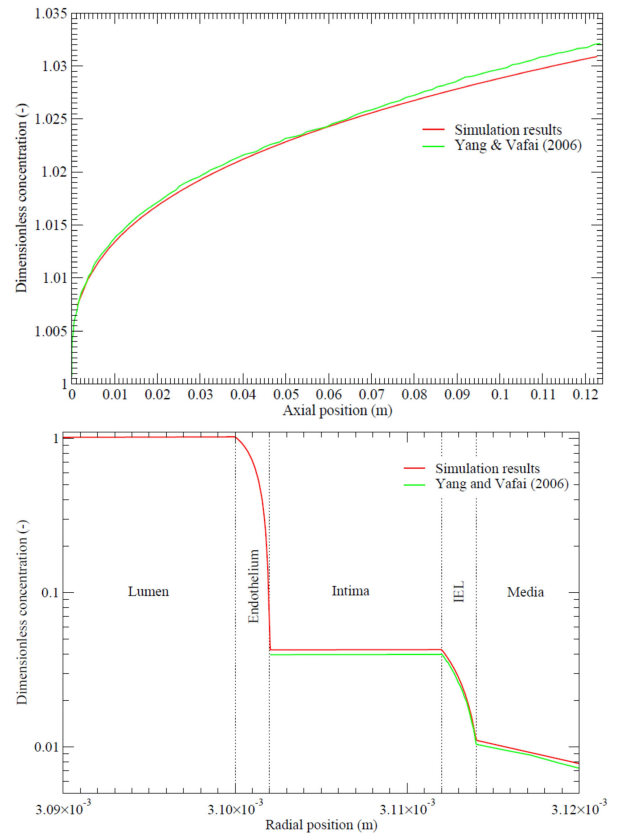


Fig. 2: Profiles of the dimensionless LDL concentration at the lumen-endothelium interface (-top) and in the artery wall (-bottom). Comparison with results obtained in [4] for a simple cylinder geometry.

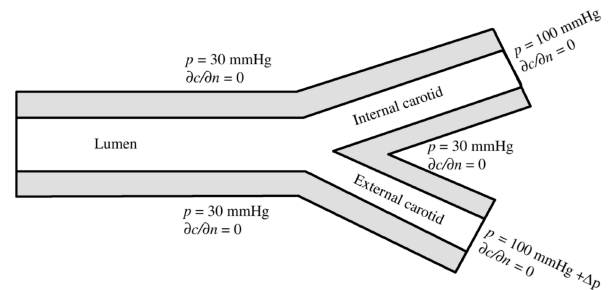


Fig. 3: The boundary conditions for the carotid bifurcation. The pressure difference between outlets is indicated by Δp . The size is not to scale.

tude within the artery wall at 0.062 m behind the artery inlet of $v=2.29 \times 10^{-8}$ m/s show a very good agreement with results of [4] where a value of $v=2.31 \times 10^{-8}$ m/s is reported. The effect of the concentration polarisation at the lumen-endothelium interface is clearly visible, Fig. 2-top. This proved a proper implementation of the multi-layered

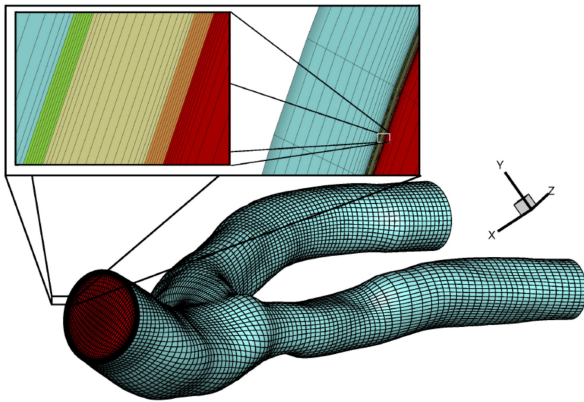


Fig. 4: The computational mesh used in simulations of the patient-specific carotid bifurcation. The lumen is indicated in red, the endothelium in orange, the intima in yellow, the internal elastic layer (IEL) in green and the media in blue.

artery wall mathematical model.

Next, we move to the patient-specific carotid artery bifurcation. The boundary conditions for this patient-specific geometry are shown in Fig. 3. The pressure boundary conditions are applied at outlets to ensure recorded 0.6:0.4 (internal/external carotid artery) mass-flow ratios, [5]. The fully developed laminar flow profile with an average velocity of $v=0.06$ m/s is imposed at the inlet, which gives a typical Reynolds number of $Re=105$. Despite the constant thickness assumption, due to a high aspect ratio between different layers, it is quite challenging to generate the patient-specific numerical mesh of a good quality for the considered problem. To be able to capture the expected large gradients of the LDL concentration in the endothelium and IEL layers, a refined numerical mesh must be applied in these regions. The computation mesh that includes the lumen and artery wall layers is shown in Fig. 4. At least 8 CVs are required to properly resolve the endothelium and IEL layers. The final numerical mesh consists from approximately 2×10^6 hexagonal control volumes that was proven to be sufficient to obtain a grid-independent result (with a second-order quadratic upwind discretisation scheme for velocity and concentration convective terms). Note that endothelium and IEL layers are treated as biological membranes, i.e. the osmotic pressure term in Eq.(1) is taken into account for these layers. The uptake of LDL in the tissue is modelled using a first-order chemical reaction. The chemical reaction sink term is active only in the media, $k_{react} = -3.197 \times 10^{-4}$ 1/s. The parameters used in simulations are the same as proposed in [4]. For reflection coefficients in the intima and media, values proposed by [6] are used. Instead of solving flow and mass transport in the adventitia a simple zero-gradient boundary condition is imposed at

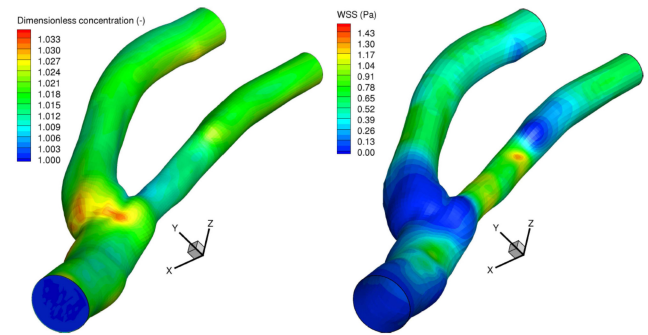


Fig. 5: Dimensionless LDL concentration (c/c_0) at the endothelium-intima interface (-left) and wall-shear-stress (WSS) along the artery wall (-right).

the media/adventia interface. The reference concentration of LDL at the inlet is $c_0=0.0286$ mol/m³. An isothermal system is assumed with a reference temperature of 37⁰C.

Contours of the dimensionless LDL concentration and wall-shear-stress (WSS) along the artery wall are shown in Fig. 5. It can be seen that a maximum increase of 3.5% of the LDL concentration is obtained at the carotid sinus, Fig. 5-left. This corresponds to the region where a low WSS is obtained, as shown in Fig. 5-right. It can be concluded that a strong correlation between high local LDL concentration and low WSS region exist. The concentration polarisation is nicely illustrated in Fig. 6, where contours of the dimensionless LDL concentration are shown in different intersections. It is clear that the thickness of the polarisation layer is not constant, i.e. there is a strong dependency between blood flow patterns and distributions of the LDL concentration in the lumen, which will influence the uptake of the LDL in the artery wall. The profiles of the LDL concentration at two characteristic locations in the artery wall are shown in Fig. 7. Despite the qualitative similarity in the radial distributions with strong gradients within the endothelium and IEL and approximately linear decrease in the media, the LDL concentration distributions clearly show some important differences too. At the first location, in the proximity of the carotid sinus, Fig. 7-top, the value of the LDL concentration in the intima is twice as high as compared to the second location that is placed more downstream at the external carotid artery, Fig. 7-bottom. Similarly, the LDL concentration values at the media/adventia interface show significantly higher values at the first location.

IV. CONCLUSIONS

It is demonstrated that a multi-layer wall model for transport of the LDL through the artery wall, proposed by Yang and Vafai [4] and tested on relatively simple two-

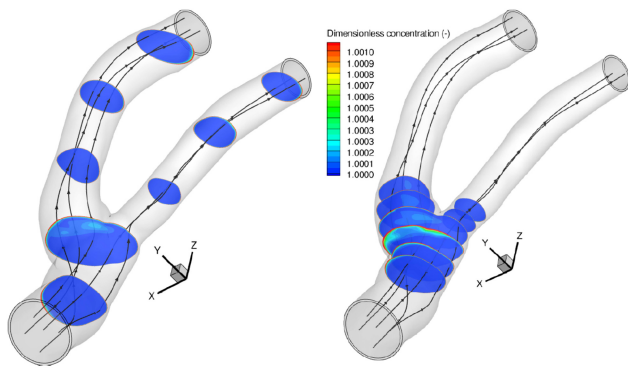


Fig. 6: Contours of the LDL concentration in the lumen along the carotid bifurcation (-left) and in the proximity of the carotid sinus (-right).

dimensional geometries, can be successfully applied to the patient-specific carotid artery case. Despite challenging requirements in terms of the relatively complex mesh generation and relatively high number of required transport parameters for each particular layer, it is concluded that the four-layer (endothelium-IEL-intima-media) wall model represents a good basis for the future numerical investigations of atherosclerosis development for the patient-specific conditions.

ACKNOWLEDGEMENTS

Dr. Frank Gijzen, Erasmus Medical Centre, Rotterdam, The Netherlands is acknowledged for providing geometry of the patient-specific carotid artery used in this study.

REFERENCES

1. De Bakey M E, Lawrie G M, Glaeser D H, Patterns of atherosclerosis and their surgical significance *Annals of Surgery* 1985, **201**(2):115-131.
2. Ross R, Atherosclerosis - an inflammatory disease *New England Journal of Medicine* 1999, **340**(2):115-126.
3. Khakpour M and Vafai K, Critical assessment of arterial transport models *Int. J. Heat and Mass Transfer* 2008, **51**:807-822.
4. Yang N and Vafai K, Modeling of low-density lipoprotein (LDL) transport in the artery - effects of hypertension *Int. J. Heat and Mass Transfer* 2006, **49**:850-867.
5. Groen H C, Simons L, van den Bouwhuijsen Q J A, Bosboom E M H, Gijzen F J H, van der Giessen A G, van de Vosse F N, Hofman A, van der Steen A F W, Witteman J C M, van der Lugt A and Wentzel J J, MRI-based quantification of outflow boundary conditions for computational fluid dynamics of stenosed human carotid arteries *Journal of Biomechanics* 2010, **43**(12):2332-2338.
6. Prosi M, Zunino P, Perktold K and Quarteroni A, Mathematical and numerical models for transfer of low-density lipoproteins through the arterial walls: a new methodology for the model set up with applications to the study of disturbed luminal flow *Journal of Biomechanics* 2005, **38**:903-917.

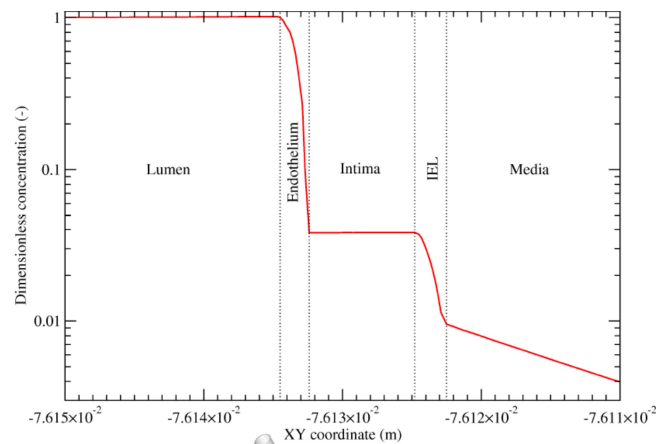
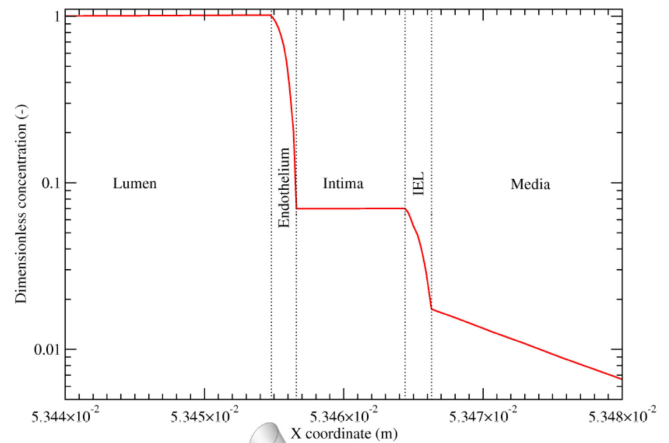


Fig. 7: Profiles of the LDL concentration at several locations (indicated by the red dots) in the artery wall.

Author: Dr. Saša Kenjereš
 Institute: Faculty of Applied Sciences, Delft University of Technology
 Street: Leeghwaterstraat 39, 2628 CB
 City: Delft
 Country: The Netherlands
 Email: S.Kenjeres@tudelft.nl